Origin of Structural Modulations in Ultrathin Fe Films on Cu(001)

Xie Zhang,[1,*] Tilmann Hickel,[1] Jutta Rogal,[2] and Jörg Neugebauer[1]
[1]*Max-Planck-Institut für Eisenforschung GmbH, 40237 Düsseldorf, Germany*
[2]*Interdisciplinary Centre for Advanced Materials Simulation, Ruhr-Universität Bochum, 44780 Bochum, Germany*
(Received 16 November 2016; published 9 June 2017)

Employing *ab initio* calculations we demonstrate that the complex structural modulations experimentally observed in ultrathin Fe films on Cu(001) originate from Fe bulk phases that arise under extreme deformations. Specifically, we show that the structural modulations correspond to the motifs observed when transforming fcc Fe to bcc Fe in the Pitsch orientation relationship $[(001)_{\mathrm{fcc}}||(1\bar{1}0)_{\mathrm{bcc}}]$. The observed structural equivalence between surface and unstable bulk structures naturally explains the experimentally reported magnetic and structural transitions when going from low (two to four MLs) to intermediate (four to ten MLs) film coverages.

DOI: 10.1103/PhysRevLett.118.236101

Ultrathin Fe films have attracted a lot of attention as a prototype system to study the interplay between magnetism and structure [1–21]. One of the driving forces for these works is the desire to study face-centered cubic (fcc) Fe, which as a bulk phase is thermodynamically unstable at room temperature. Specifically, its bulk phase is only stable at temperatures between 1185 and 1667 K in a paramagnetic state [22], while at low temperatures it is stable in a ferromagnetic (FM) body-centered cubic (bcc) structure. Using molecular beam epitaxy [23] experimentalists aimed to grow ultrathin fcc Fe films on Cu(001) that are stable even at low temperatures (e.g., 300 K). The concept appeared very promising since Cu is stable in fcc structure and its lattice constant is close (lattice mismatch $< 1\%$) to that of bulk fcc Fe.

Despite the fundamental concept being highly intuitive, interpreting the magnetic and structural behavior of the films has challenged both experimentalists and theoreticians for decades. Combining various experimental techniques, three regions showing distinct magnetic and structural features with respect to the coverage (i.e., number of MLs N) were identified. As sketched in Fig. 1(b), in region I ($1 < N \lesssim 4$ MLs), the film has a FM ordering [5,9,13] and a large lattice modulation [11]. Specifically, the high-symmetry Fe(001) surface reduces its symmetry by forming stripes along the $[1\bar{1}0]$ direction with repeating "fcc-like" [12] or "bcc-like" [17] motifs [Fig. 1(a)]. These periodic patterns on the surface have been termed modulations. Experiments showed that they are not restricted to the surface layer(s), but extend through the entire film [11]. In region II ($4 < N \lesssim 10$ MLs), the Fe film shows a magnetic transition to an antiferromagnetic (AFM) state [5,10,13]. Moreover, a surface reconstruction [9] and a FM coupling of the top two layers [14] were observed. In region III ($N \gtrsim 10$ MLs), the nucleation of bcc clusters and a plastic relaxation at the interface start to appear [16,17] and eventually drive the entire film to transform to the bulk ground state, i.e., FM bcc Fe [9,16,17].

From a theoretical perspective, *ab initio* approaches are routinely employed to study surface reconstructions. However, identifying the modulated structures in the current system is challenging: experiments showed that FM fcc Fe thin films are unstable even on Cu(001) (e.g., Ref. [11]). Because of the high symmetry of the unperturbed surface, the lateral forces on the atoms are zero. Consequently, straightforward force relaxations cannot yield the stable structures. Motivated by the experimental observations, Spišák and Hafner [20] developed an approach by laterally displacing the fcc Fe atoms in a (1×4) surface unit cell [relative to the primitive one of fcc (001) Fe] along the $\pm[110]$ directions, constraining the atoms in deeper layers to relax only along the $[110]$ and $[001]$ directions. With this method, modulated structures

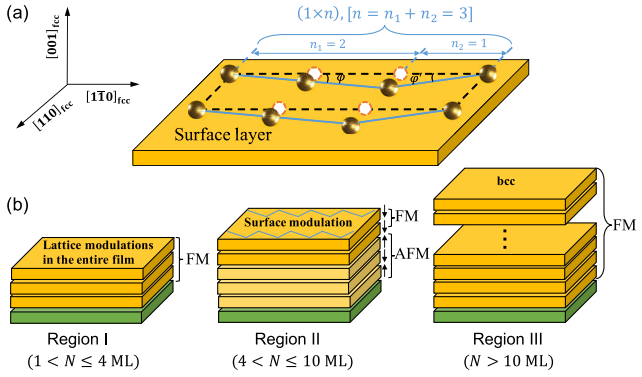

FIG. 1. (a) Schematic illustration of the $(1 \times n), [n = n_1 + n_2]$ modulations in ultrathin Fe films on Cu(001). In the current example, $n = 3$ with $n_1 = 2$ and $n_2 = 1$. φ and $-\varphi\prime$ are defined as shear angles relative to the primitive cell of fcc(001) Fe. The gold spheres refer to the Fe atoms on the surface and the open circles indicate the original positions of the Fe atoms on fcc(001) Fe. (b) Structural and magnetic features of three distinct regions observed in experiments. The green layer denotes the Cu substrate and the orange layers represent the Fe layers. The AFM Fe layers are shaded by light orange.

corresponding to local energy minima were successfully identified, which significantly improved the structure model of the films. A missing piece of these surface calculations is the identification of the underlying fundamental mechanisms and structural motifs that drive these complex modulations.

Recent scanning tunneling microscopy experiments by Biedermann *et al.* [24,25] suggest that lattice modulations in region I result from a phase transition and termed the modulated structure nanomartensite. This opens a new perspective and suggests that the film structures may be viewed as metastable or unstable bulk phases. Such phases may never be observed for the free bulk but may be stabilized by the epitaxial relation with the substrate. The key idea of the present study is to start from identifying metastable or unstable bulk phases that are between the two constraining structures the film likes to have, i.e., the fcc structure imposed by the substrate and the bcc structure that is the thermodynamic ground state. The idea is then to look at intermediate phases that arise along the diffusionless (bulk) fcc → bcc transition paths.

Since the fcc → bcc transition plays a key role in metallurgy, various transition paths have been studied [26]. The various paths can be classified by the orientation relationship (OR), which specifies the orientation the crystal has before and after the transition. For the present case the orientation of the fcc phase is dictated by the Cu(001) substrate. This constraint is compatible with the Bain OR $[(001)_{\mathrm{fcc}}||(001)_{\mathrm{bcc}}]$ or the Pitsch OR $[(001)_{\mathrm{fcc}}||(1\bar{1}0)_{\mathrm{bcc}}]$ [27]. As shown by various theoretical studies, the Bain path exhibits no metastable intermediate configurations between fcc Fe and bcc Fe (see, e.g., Ref. [28]). The transition path in the Pitsch OR has been studied recently by *ab initio* calculations [29,30]. This study revealed a hitherto unknown intermediate structure. We will use this prior knowledge to reduce the high-dimensional configuration space of possible film structures and to identify their generic structural motifs.

We first investigate the effect of the lateral constraint [31] induced by the Cu substrate on the recently identified bulk fcc → bcc Fe transition path that shows the metastable intermediate structure. Specifically, we perform solid-state nudged elastic band simulations [32] as implemented in the VTST code [33,34] using energies and forces computed from density-functional theory (see Ref. [35]) with the same parameter setup to calculate the minimum energy path (MEP). The path is sampled for the FM state that is the magnetic configuration for the region where the modulated structures are observed.

The fully relaxed (lattice constants, cell shape, and atomic positions) MEP (blue line) reveals a local minimum between fcc Fe and bcc Fe (Fig. 2). The structure corresponding to the local minimum is formed by displacing the atoms along a sinusoidal line. The resulting modulation is shown in the bottom left inset in Fig. 2 (light blue dashed line and arrows). We call the modulated

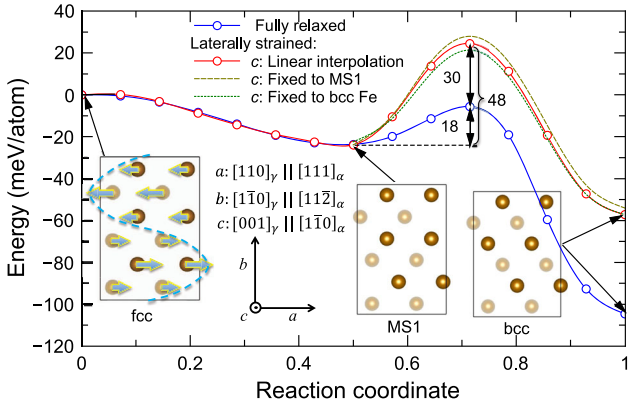

FIG. 2. Minimum energy paths of the FM fcc → bcc Fe transition in the Pitsch OR. The reaction coordinate is normalized to 1 with images equally distributed along the path. The orthorhombic unit cells (12 atoms) for fcc, bcc, and MS1 are shown as insets. The atoms are visualized by gold spheres and shaded based on the depth of the atoms in the c direction. The light blue arrows show the displacements of Fe atoms to transform from fcc Fe to MS1. The resulting modulation is sketched by the light blue dashed line.

structure identified here MS1, since we will later show the existence of another modulated structure (MS2). The transition from fcc Fe to MS1 is barrier free [47], while there is an energy barrier of ∼18 meV/atom for the MS1 → bcc transition. Since the optimized lattice constants c of epitaxially constrained fcc, bcc, and MS1 are slightly different (see Ref. [35]), and due to the technical limitation to relax the vertical lattice constant while fixing the lateral one in nudged elastic band calculations, we use a linear interpolation of the lattice constant c along the path. To check the reliability of this assumption, we consider two limiting cases by fixing the lattice constant c to that of either MS1 or bcc Fe. As shown in Fig. 2, the resulting paths are very similar (dark yellow and green dashed lines), validating the chosen approach. Hence, even if we take into account the epitaxial constraint, MS1 remains as an intermediate state along the path, but the energy barrier for the transition to bcc Fe increases by ∼30 meV/atom (i.e., becomes ∼48 meV/atom).

Since we only explore the potential energy surface (PES) of the fcc → bcc Fe transition path along a one-dimensional reaction coordinate, from the fact that it shows a local minimum we cannot conclude that MS1 is metastable. To check this we compute the dynamical matrix of MS1 (see Ref. [35]). The resulting phonon spectrum reveals imaginary modes, implying that MS1 is unstable and only a saddle point on the full $3N_{\mathrm{atom}}$ (N_{atom} = number of atoms) dimensional PES. Enforcing the epitaxial constraint by the Cu substrate, the number of imaginary modes decreases but the one around the Γ point remains. Collectively displacing all atoms along the corresponding eigenvector of the imaginary phonon mode at the Γ point, we find an energetically more stable structure that we name MS2. The phonon dispersions of MS2 show that this structure is dynamically stable for both the epitaxially

constrained and the fully relaxed cases. Notably, our further calculations will show that MS1, which is unstable in the bulk, becomes stable on the surface. Hence, we consider both MS1 and MS2 as potential structural candidates for the Fe films.

Both fcc-like and bcc-like have been used to describe the experimentally observed local structural features of the modulated structures (e.g., Ref. [12,17]). We herewith show how the above discovered new structures help to resolve these inconsistencies. Figure 3 shows a top view of the fully relaxed fcc, MS1, MS2, and bcc surfaces. For fcc or bcc surfaces, only one structural motif (yellow boxes labeled F and B, respectively) is needed to form the entire surface. MS1 consists of three types of fcc-like or bcc-like stripes, namely, F, B_{φ}, and $B_{\varphi\prime}$ [Fig. 3(b)]. The stripe F in MS1 is slightly distorted and is thus, precisely speaking, fcc-like rather than fcc. Consistent with Fig. 1(a), the bcc-like stripes B_{φ} and $B_{-\varphi\prime}$ are characterized by the shear angles relative to the primitive cell of fcc(001) Fe, i.e., φ and $-\varphi\prime$. The two shear angles in MS1 are $\pm 13°$, respectively, which are smaller (in absolute value) than the original shear angle of 19° in bcc Fe [Fig. 3(d)]. MS2 is composed of bcc-like stripes only.

The above introduced fcc-like and bcc-like stripes can be considered as the basic structural motifs for the ultrathin Fe films on Cu(001). Specifically, the experimentally observed $(1 \times n)$ modulations in the Fe films as shown in Fig. 1(a) can be constructed by a combination of n_1 B_{φ} and n_2 $B_{\varphi\prime}$ stripes, where φ and $\varphi\prime$ need to fulfill the geometric relation, i.e., $\tan\varphi/\tan\varphi\prime = n_2/n_1$. More complex modulations that include the fcc-like motif [e.g., the (1×3) modulation in Fig. 3(b)] can be constructed by combining the structural motif F with motifs B_{φ} and $B_{-\varphi\prime}$.

Having identified the basic structural motifs, we can systematically explore different types of structural modulations in the ultrathin Fe films on Cu(001). To construct the complete phase diagram, one needs to consider three key variables, namely, surface structures, the coverage, and the magnetic configuration. In order to demonstrate the principle of this approach, we herewith focus on the two modulated structures identified above, considering different coverages and magnetic configurations as

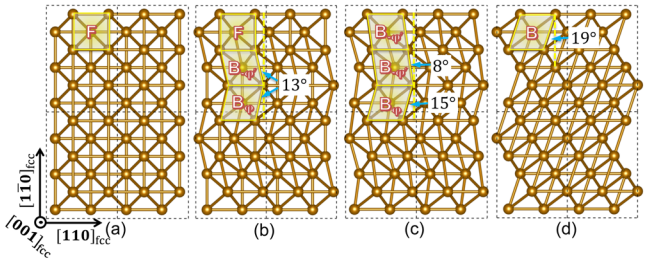

FIG. 3. Top view of the various surface structures: (a) fcc, (b) MS1, (c) MS2, and (d) bcc. The yellow shaded boxes with labels F and B_{φ} (or $B_{-\varphi\prime}$) indicate the fcc-like or bcc-like structural motifs in the modulated structures, respectively. The black dashed lines show the (2×3) unit cell as the reference.

reported in the literature [15,48–51]. Note that magnetic transitions from out-of-plane to in-plane magnetizations with increasing film thickness have been reported (e.g., Ref. [9]). However, this mainly occurs at larger thicknesses where the film has transformed to FM bcc Fe. Since this effect results only in a small decrease of the energy (on the order of 0.1 meV/atom [52]) of the bcc phase, it is not considered in this study. As shown in the following, this limited set of structures reproduces the three distinct regions [Fig. 1(c)] observed in experiment. Convergence checks by inspecting the energy difference between structures with varied thickness (three to five MLs) of the Cu substrate show that the main effect of the Cu substrate layers is to keep the lateral lattice constant of bulk Cu. Hence, we use only three MLs of fcc Cu as the substrate and add one to eight MLs of fcc, MS1, MS2, or bcc Fe (see Ref. [35]). After careful tests to ensure a convergence of the total energy to an error of ≤ 0.2 meV/Fe atom, the thickness of the vacuum is set to 12 Å. The bottom layer of Cu is fixed, while the other Cu and Fe layers are allowed to fully relax using density-functional theory (residual forces ≤ 0.001 eV/Å). Intermixing between the epitaxial ultrathin Fe films and the substrate has been reported both experimentally [53] and theoretically [54]. As shown in Refs. [55,56], the overall magnetic states and structural patterns of the films are insensitive to the intermixing. Hence, we restrict this study to atomically abrupt interfaces. The AFM phases are described using collinear AFM configurations as suggested in Ref. [15]. Notably, nonmagnetic Fe films always relax to fcc Fe and are energetically much higher than the magnetic films. Hence, we only discuss the structures of the magnetic films. The results of these calculations are summarized in Fig. 4 and will be discussed in the following.

As shown in Fig. 4(a1), when the coverage is below four MLs, the Fe film energetically favors the FM modulated structures. As an extreme case, a one-ML Fe film always relaxes to the fcc structure of the Cu substrate irrespective of the starting modulation. For two- and three-ML films the modulations extend through the entire film. The shear angles on the surfaces of FM MS1 and MS2 become 15° and 14°, respectively, which are consistent with experiment, 14° [17,25]. Notably, FM MS1 and MS2 are both stable and energetically almost degenerate, implying that combinations of the three structural motifs (F, B_{φ}, and $B_{-\varphi\prime}$ in Fig. 3) are energetically favorable, resulting in more complex modulations as indeed observed in experiment. Hence, the key features of region I ($1 < N < 4$ MLs) [Fig. 4(a1)] are (i) the film is FM, and (ii) the modulation extends through the entire film.

When the coverage is four to seven MLs, the AFM MS1 becomes energetically competitive. For all favorable AFM configurations, a FM coupling for the top two layers is found. To analyze the impact of the magnetic configuration

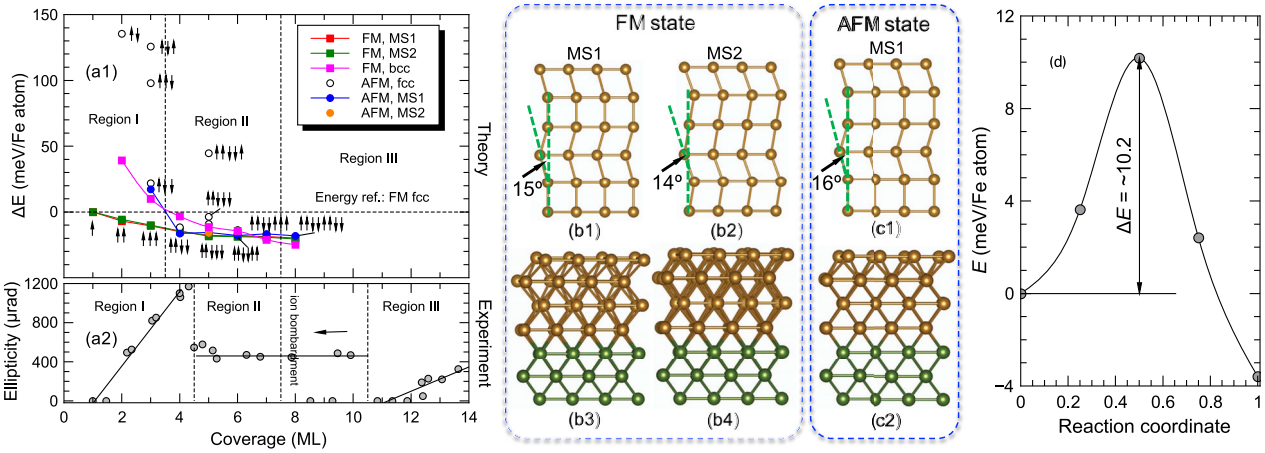

FIG. 4. (a1) Energy of ultrathin Fe films on Cu(001) as a function of coverage considering different structures and magnetic states (the layer magnetization is indicated by uparrow and downarrow). The energy is defined as the difference from the FM fcc film with an identical thickness normalized by the number of Fe atoms [57]. (a2) Experimental thickness dependence of the Kerr ellipticities (reproduced from Ref. [9]), clearly indicating three regions. The vertical dashed lines denote the critical thicknesses for transitions between two regions. The lower boundary of region III is reduced to eight MLs after ion bombardment [58–60]. (b1),(b2) Surface structures (top view) of the four-ML films in the FM state with MS1 and MS2, respectively. (b3),(b4) Side views of the FM films. (c1), (c2) The film structures in the AFM state. The gold spheres refer to Fe atoms, while the green ones represent Cu atoms. (d) Minimum energy path of the FM MS1 → FM bcc Fe (representatively, five MLs) transition on Cu(001).

on the modulation we compare in Figs. 4(b1)–4(b4) and Figs. 4(c1) and 4(c2) the structure of a four-ML film for a FM and an AFM configuration. Specifically, the modulations in the surface layer are almost identical. However, the extension through the film is qualitatively different: while for the FM case it extends through the entire film, it is for the AFM case restricted to the top surface layer. The modulations are therefore intrinsically coupled to the presence of a FM spin orientation.

Since the FM and AFM phases are almost degenerate, the magnetism in the deeper layers will be a mixture of FM and AFM states. This mixture results in a partial demagnetization of the film consistent with experiment [61]. Our surface phonon calculation of the FM MS1 further confirms that it is dynamically stable, though it is unstable in the bulk. MS2 is always unstable and relaxes to MS1 for AFM states. This finding immediately explains why experimentally only a (1×2) reconstruction was observed in region II, while several kinds of reconstructions were observed in region I. The basic features of region II ($4 \leq N \leq 7$ MLs) [Fig. 4(a1)] can be summarized as (i) the modulation only occurs in the top surface layer, and (ii) to stabilize the modulation, the top two surface layers must have FM coupling, while the magnetic configuration of the lower layers is no longer purely FM.

Starting at eight MLs the FM bcc phase (purple line) becomes energetically most stable. The early crossover looks like a contradiction to experiment where this phase is only observed for thicknesses larger than ten MLs. We speculate that the transition from the modulated structures to bcc Fe is not barrier free, i.e., the critical thickness at which the transition occurs will be shifted to larger thicknesses. Indeed, the existence of a barrier is supported by our calculated MEP [Fig. 4(d)], where a barrier of ~10 meV/Fe atom is found. We expect that this barrier stabilizes MS1 and expands the window of region II. This hypothesis is supported by experiment: ion bombardment triggers this transition already at eight MLs [58–60] [Fig. 4(a2)], consistent with the predicted one.

To conclude, the complex structural modulations experimentally observed in ultrathin Fe films on Cu(001) can be consistently and physically intuitively described by transferring the insight from a recently discovered fcc → bcc Fe transition path. This path, in contrast to the established ones, shows an intermediate phase that allows us to systematically construct low energy structures for the Fe films. Using this approach, we are able to interpret the complex lattice modulations and surface reconstructions in terms of three structural motifs, and explain the structural and magnetic features of the experimentally observed regions in the films. The concept employed here to use information from the bulk transition paths together with ORs compatible with the specific substrate surface is general and expected to provide a valuable tool in the study and identification of surface structures of metallic thin films that undergo martensitic transitions. Possible candidates are magnetic shape memory alloys such as Fe-Pd, Fe-Pt, and Ni-Mn-Ga.

We gratefully acknowledge financial support of the Deutsche Forschungsgemeinschaft (DFG) within the collaborative research center SFB761 “Stahl-*ab initio*.”

*Corresponding author.
x.zhang@engineering.ucsb.edu

[1] B. T. Jonker, K.-H. Walker, E. Kisker, G. A. Prinz, and C. Carbone, Phys. Rev. Lett. **57**, 142 (1986).
[2] P. A. Montano, G. W. Fernando, B. R. Cooper, E. R. Moog, H. M. Naik, S. D. Bader, Y. C. Lee, Y. N. Darici, H. Min, and J. Marcano, Phys. Rev. Lett. **59**, 1041 (1987).
[3] D. A. Steigerwald and W. F. Egelhoff, Jr., Phys. Rev. Lett. **60**, 2558 (1988).
[4] W. Daum, C. Stuhlmann, and H. Ibach, Phys. Rev. Lett. **60**, 2741 (1988).
[5] W. A. A. Macedo and W. Keune, Phys. Rev. Lett. **61**, 475 (1988).
[6] D. P. Pappas, K.-P. Kämper, and H. Hopster, Phys. Rev. Lett. **64**, 3179 (1990).
[7] H. Magnan, D. Chandesris, B. Villette, O. Heckmann, and J. Lecante, Phys. Rev. Lett. **67**, 859 (1991).
[8] R. Allenspach and A. Bischof, Phys. Rev. Lett. **69**, 3385 (1992).
[9] J. Thomassen, F. May, B. Feldmann, M. Wuttig, and H. Ibach, Phys. Rev. Lett. **69**, 3831 (1992).
[10] D. Li, M. Freitag, J. Pearson, Z. Q. Qiu, and S. D. Bader, Phys. Rev. Lett. **72**, 3112 (1994).
[11] S. Müller, P. Bayer, C. Reischl, K. Heinz, B. Feldmann, H. Zillgen, and M. Wuttig, Phys. Rev. Lett. **74**, 765 (1995).
[12] R. D. Ellerbrock, A. Fuest, A. Schatz, W. Keune, and R. A. Brand, Phys. Rev. Lett. **74**, 3053 (1995).
[13] D. J. Keavney, D. F. Storm, J. W. Freeland, I. L. Grigorov, and J. C. Walker, Phys. Rev. Lett. **74**, 4531 (1995).
[14] M. Straub, R. Vollmer, and J. Kirschner, Phys. Rev. Lett. **77**, 743 (1996).
[15] T. Asada and S. Blügel, Phys. Rev. Lett. **79**, 507 (1997).
[16] A. Biedermann, M. Schmid, and P. Varga, Phys. Rev. Lett. **86**, 464 (2001).
[17] A. Biedermann, R. Tscheließnig, M. Schmid, and P. Varga, Phys. Rev. Lett. **87**, 086103 (2001).
[18] D. Qian, X. F. Jin, J. Barthel, M. Klaua, and J. Kirschner, Phys. Rev. Lett. **87**, 227204 (2001).
[19] S. S. A. Razee, J. B. Staunton, L. Szunyogh, and B. L. Gyorffy, Phys. Rev. Lett. **88**, 147201 (2002).
[20] D. Spišák and J. Hafner, Phys. Rev. Lett. **88**, 056101 (2002).
[21] T. Bernhard, M. Baron, M. Gruyters, and H. Winter, Phys. Rev. Lett. **95**, 087601 (2005).
[22] L. Kaufman, E. Clougherty, and R. Weiss, Acta Metall. **11**, 323 (1963).
[23] J. R. Arthur, Surf. Sci. **500**, 189 (2002).
[24] A. Biedermann, R. Tscheließnig, M. Schmid, and P. Varga, Appl. Phys. A **78**, 807 (2004).
[25] A. Biedermann, Phys. Rev. B **80**, 235403 (2009).
[26] Z. Nishiyama, *Martensitic Transformations* (Elsevier, Amsterdam, 2012).
[27] W. Pitsch, Philos. Mag. **4**, 577 (1959).
[28] M. Friák, M. Šob, and V. Vitek, Phys. Rev. B **63**, 052405 (2001).
[29] X. Zhang, T. Hickel, J. RogalS. Fähler, R. Drautz, and J. Neugebauer, Acta Mater. **99**, 281 (2015).
[30] X. Zhang, T. Hickel, J. Rogal, and J. Neugebauer, Phys. Rev. B **94**, 104109 (2016).
[31] The lateral strain on the (a, b) plane is around -0.05% relative to FM fcc Fe.
[32] D. Sheppard, P. Xiao, W. Chemelewski, D. D. Johnson, and G. Henkelman, J. Chem. Phys. **136**, 074103 (2012).
[33] G. Henkelman and H. Jónsson, J. Chem. Phys. **113**, 9978 (2000).
[34] D. Sheppard, R. Terrell, and G. Henkelman, J. Chem. Phys. **128**, 134106 (2008).
[35] See Supplemental Material at http://link.aps.org/supplemental/10.1103/PhysRevLett.118.236101 for computational details, the phonon dispersions of the modulated structures, the complete properties of the relevant structures, as well as the structural setup for the ultrathin Fe films on Cu(001), which includes Refs. [36–46].
[36] P. E. Blöchl, Phys. Rev. B **50**, 17953 (1994).
[37] J. P. Perdew, K. Burke, and M. Ernzerhof, Phys. Rev. Lett. **77**, 3865 (1996).
[38] P. Söderlind and A. Gonis, Phys. Rev. B **82**, 033102 (2010).
[39] G. Kresse and J. Furthmüller, Phys. Rev. B **54**, 11169 (1996).
[40] H. J. Monkhorst and J. D. Pack, Phys. Rev. B **13**, 5188 (1976).
[41] M. Methfessel and A. T. Paxton, Phys. Rev. B **40**, 3616 (1989).
[42] S. Boeck, C. Freysoldt, A. Dick, L. Ismer, and J. Neugebauer, Comput. Phys. Commun. **182**, 543 (2011).
[43] C. S. Roberts, Trans. AIME **197**, 203 (1953).
[44] A. Udyansky, J. von Pezold, A. Dick, and J. Neugebauer, Phys. Rev. B **83**, 184112 (2011).
[45] D. E. Jiang and E. A. Carter, Phys. Rev. B **67**, 214103 (2003).
[46] N. I. Medvedeva, D. Van Aken, and J. E. Medvedeva, J. Phys. Condens. Matter **22**, 316002 (2010).
[47] Precisely speaking and the structure is already face-centered tetragonal due to the tetragonal distortion in the FM state.
[48] R. Lorenz and J. Hafner, Phys. Rev. B **54**, 15937 (1996).
[49] D. Spišák and J. Hafner, Phys. Rev. B **61**, 16129 (2000).
[50] D. Spišák and J. Hafner, Phys. Rev. B **66**, 052417 (2002).
[51] M. Marsman and J. Hafner, Phys. Rev. B **66**, 224409 (2002).
[52] Y.-C. Lin, C.-B. Wu, W.-S. Li, Y.-C. Chen, Z.-Y. Huang, W.-C. Lin, and M.-T. Lin, Appl. Phys. Express **7**, 23005 (2014).
[53] H. L. Meyerheim, R. Popescu, D. Sander, J. Kirschner, O. Robach, and S. Ferrer, Phys. Rev. B **71**, 035409 (2005).
[54] S. Lee and Y. Chung, Jpn. J. Appl. Phys. **46**, 6309 (2007).
[55] D. Spišák and J. Hafner, Phys. Rev. B **64**, 205422 (2001).
[56] H. Zenia, S. Bouarab, and C. Demangeat, Surf. Sci. **521**, 49 (2002).
[57] In the case of FM bcc Fe, an entropy induced energy difference of 10 meV/Fe atom at 300 K as computed in Ref. [25] is included. Notably, Ref. [25] shows that the entropy difference between fcc Fe and MS1 and MS2 is negligible, which demonstrates that it is less important to consider the temperature effects in regions I and II.
[58] W. Rupp, A. Biedermann, B. Kamenik, R. Ritter, C. Klein, E. Platzgummer, M. Schmid, and P. Varga, Appl. Phys. Lett. **93**, 063102 (2008).
[59] S. S. Zaman, P. Dvořák, R. Ritter, A. Buchsbaum, D. Stickler, H. P. Oepen, M. Schmid, and P. Varga, J. Appl. Phys. **110**, 024309 (2011).
[60] J. Gloss, S. S. Zaman, J. Jonner, Z. Novotny, M. Schmid, P. Varga, and M. Urbánek, Appl. Phys. Lett. **103**, 262405 (2013).
[61] H. L. Meyerheim, J. M. Tonnerre, L. Sandratskii, H. C. N. Tolentino, M. Przybylski, Y. Gabi, F. Yildiz, X. L. Fu, E. Bontempi, S. Grenier, and J. Kirschner, Phys. Rev. Lett. **103**, 267202 (2009).